

# Journal Pre-proof

OxGamma: A MATLAB based application for the analysis of gamma-ray spectra

R. Kumar, M. Frouin, J. Gazack, J.-L. Schwenninger

PII: S1350-4487(22)00055-5

DOI: <https://doi.org/10.1016/j.radmeas.2022.106761>

Reference: RM 106761

To appear in: *Radiation Measurements*

Received Date: 1 December 2021

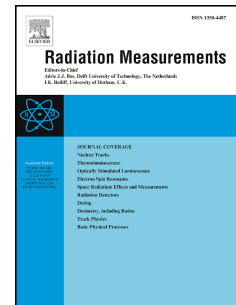
Revised Date: 17 April 2022

Accepted Date: 19 April 2022

Please cite this article as: Kumar, R., Frouin, M., Gazack, J., Schwenninger, J.-L., OxGamma: A MATLAB based application for the analysis of gamma-ray spectra, *Radiation Measurements* (2022), doi: <https://doi.org/10.1016/j.radmeas.2022.106761>.

This is a PDF file of an article that has undergone enhancements after acceptance, such as the addition of a cover page and metadata, and formatting for readability, but it is not yet the definitive version of record. This version will undergo additional copyediting, typesetting and review before it is published in its final form, but we are providing this version to give early visibility of the article. Please note that, during the production process, errors may be discovered which could affect the content, and all legal disclaimers that apply to the journal pertain.

© 2022 Published by Elsevier Ltd.



## **OxGamma: a MATLAB based application for the analysis of gamma-ray spectra**

Kumar, R.<sup>1\*</sup>, Frouin, M.<sup>2</sup>, Gazack, J. <sup>1</sup>, Schwenninger, J.-L. <sup>1</sup>

<sup>1</sup>Oxford Luminescence Dating Laboratory, RLHA, School of Archaeology, University of Oxford, OX13TG, UK

<sup>2</sup>Department of Geosciences, University of Stony Brook, NY 11794-21, USA

\*Corresponding Author: [raju.kumar@arch.ox.ac.uk](mailto:raju.kumar@arch.ox.ac.uk); [rajcelos.isp65@gmail.com](mailto:rajcelos.isp65@gmail.com)

Gamma-ray spectrometry is a well-established technique which enables to perform qualitative and quantitative analyses of gamma-ray emitting radionuclides. In trapped charge dating, portable spectrometers can be used to acquire spectra in the field, allowing for the assessment of radionuclide concentrations and hence the determination of dose rates at the exact location where samples are collected for dating. Accurate assessment of concentrations and dose rates demands proper energy, width, and efficiency calibration of the instrument by comparison against one or several radioactive standards. The 'Oxford blocks' which consist of four concrete cubes doped with known concentrations of potassium [K-block], thorium [Th-block], and uranium [U-block], as well as a background [BG-block], were constructed for this purpose and have become widely adopted by researchers for calibrating their instruments. For inexperienced users, the calibration of detectors and the analysis of field spectra for determining the concentration of radionuclides can be a challenging and laborious task that often involves multiple steps (e.g., downloading and converting data files, peak identification and selection, energy calibration, true full-peak area calculation, efficiency calculation, etc.). The processing of calibration spectra from the Oxford blocks is further complicated by the fact that the K-block contains only ~72% concrete and the Th-block contains a small amount of uranium. These factors must be accounted for in order to obtain accurate radionuclide concentrations and dose rates.

Here, we present a practical and user-friendly MATLAB based application (OxGamma), available as a free download for both Windows OS and macOS, intended to facilitate the calibration process of portable gamma-ray detectors and to provide a quick and efficient means for determining the concentration of radionuclides (K, U and Th) and dose rates. The

software has been tested and checked against results obtained independently and provides output using both the windows and threshold approaches. Crucially, it does not require users to possess in-depth experience in programming or gamma-spectrometry.

**Keywords:** Gamma-ray Spectrometry; Dose Rate Calculation; Radioactivity Analyses; Luminescence Dating.

## 1 Introduction

In electron spin resonance and luminescence dating, the derivation of an accurate age depends on the precise measurement of the total dose absorbed by the mineral grains such as quartz or feldspar during burial as well as the annual environmental dose rate (Aitken, 1985; Huntley et al., 1985; Ikeya, 1993; Rhodes, 2011). The total dose received by the mineral grains is the sum of an external and an internal contribution. The mineral grains receive an external dose from naturally occurring ionising radiation- alpha( $\alpha$ )-particles, beta( $\beta$ )-particles, and gamma( $\gamma$ )-rays- emitted during the decay of radionuclides of potassium (K), uranium (U), thorium (Th), and rubidium (Rb) contained in the surrounding sediment, and cosmic rays. Rubidium and Cosmic rays generally play a minor contribution. Measuring the concentrations of these radionuclides i.e. K, U, Th, and Rb combined with the use of suitable conversion factors can provide us with an accurate assessment of corresponding dose rates.

Several techniques are available for determining radionuclide concentrations including inductively coupled plasma mass and atomic emission spectrometry (ICP-MS and ICP-AES), high-resolution low-background gamma spectrometry, neutron activation analysis (NAA), and X-ray fluorescence analysis (XRF). All these methods are laboratory-based and, therefore, require special attention to the preparation and handling of samples (Gilmore, 2008; Rhodes, 2011). Alternatively, *in-situ* dose rate measurements using a highly sensitive portable gamma-ray spectrometer fitted with a NaI(Tl) or a LaBr probe, have become increasingly popular. This is particularly true for researchers working on archaeological sites where the correct evaluation of dose rate can be challenging and may require taking into account potential issues relating to the correct assessment of the external gamma dose rate (i.e. when samples need to be collected from inhomogeneous contexts or close to sedimentary boundaries or large rocks).

During the measurement, the spectrometer probe is usually placed horizontally into the sediment at the same spot where a sample was collected for dating. The gamma spectrum is recorded over a period of time generally lasting from 30 to 60 minutes. Provided the spectrometer was previously calibrated against one or several radioactive standards, any field spectra may then be processed to determine the relevant concentration of K, U, and Th and these can then be converted to dose rates.

Spectral analyses and the determination of concentrations and dose rates involve complex calculations and therefore, a thorough understanding of the subject and related tools is essential (Gilmore, 2008). Two approaches can be used to derive dose rates from the collected field spectra and these are generally referred to as the windows (Aitken, 1985) or the threshold (Murray et al., 1978) techniques. The former approach enables to determine the concentrations of K, U, and Th, which are then converted to infinite matrix dose rates. In contrast, the threshold approach results in a total dose rate with no specific information on the source of radiation. Both approaches are distinct and make use of different algorithms. In the windows approach, the first step involves the processing of calibration spectra measured from one or several radioactive standards in order to identify the correct photopeaks of interest (e.g., the photopeak at 1460 keV in a gamma spectrum reflects the emission from  $^{40}\text{K}$ ) which then enables to perform an energy calibration where individual channels are converted into energy (keV). The next step is to define the width of each photopeak for the calculation of the count rate (width calibration) and to determine the full-energy peak efficiency (efficiency calibration) as described by Gilmore (2008) and Arnold et al. (2012). Finally, following the simple procedure outlined later in this paper, the concentration of the radionuclides and corresponding dose rates can be calculated. Data analysis using the windows technique can be difficult and time-consuming and minor mistakes can result in significant uncertainty. The same can also be true for the threshold approach which requires cumulative spectra to be calculated from the measured calibration standard(s) and to determine an energy threshold for which the count rate would be proportional to dose rate (Murray et al., 1978; Mercier & Falguères, 2007).

Instrument manufacturers supply proprietary software for spectral analysis, but this can be expensive and the software is often inflexible and difficult to use. Users still need to go

through many of the required procedures and do many of the calculations before they can determine dose rates (Gilmore, 2008). Various open-source software packages are available and, more recently, dedicated functions have been written for the statistical programming language 'R' (Lebrun et al., 2020). However, deriving dose rates can still be a time-consuming task and requires familiarity with dedicated software or programming skills. Given that the data from the different radioactive standard(s) must be processed differently with some extra steps in the algorithm (e.g., calculation of the concentrations or activities of the parent radionuclides from their respective standard(s)/block(s)), it can become challenging to develop a standard piece of software or function and, for this reason, many practitioners either use or develop their own 'in-house' software tool.

In this paper, we present a user-friendly and straightforward MATLAB-based application called OxGamma. The application is available for both Windows OS and macOS and is specifically developed to permit easy and speedy calibration and calculation of the concentration of radionuclides (K, U, and Th) and dose rates from the spectra acquired in the field. OxGamma enables dose rate determination using both the windows and threshold approaches and does not require users to have previous programming experience. This software is currently available to use with the four doped concrete calibration blocks housed at the Research Laboratory for Archaeology and the History of Art, University of Oxford (Rhodes & Schwenninger, 2007). These standards known as the 'Oxford blocks', are used by many researchers to calibrate their portable instruments (Hossain, 2003; Mercier & Falguères, 2007; Arnold et al., 2012; Bates et al., 2013; Duval & Arnold, 2013; Moska et al., 2021). We also present results for some gamma-ray spectra and compare them with those obtained using in-house legacy software and ICP-MS analysis. We envisage that future updates of the software tool may include additional reference standards located in other parts of the world. In doing so, improved standardisation in the processing of calibration spectra will be possible and we hope this will help to reduce variability in the calibration methods, to avoid potential mistakes during data analysis, and to encourage inter-comparison of datasets.

## 2 Sample and instrumentation

## 2.1 Oxford calibration blocks

The 'Oxford blocks', four  $\sim 50 \text{ cm}^3$  concrete cubes, were initially constructed by Bowman, (1976) as part of her DPhil research project in order to calibrate a portable gamma-ray spectrometer. Each block has a horizontal cylindrical hole (diameter  $\sim 11 \text{ cm}$ ) running through the centre of one face to allow the detector to be inserted and positioned at the centre of the cube. Three of the four blocks were doped with known concentrations of potassium [K-block], thorium [Th-block], and uranium [U-block], and the fourth one was left undoped to use it as a background [BG-block]. According to Rhodes & Schwenninger (2007), the Th-block also contains a small portion of U ( $\text{U/Th} \sim 0.049$ ), and the K-block is only 72 % concrete (the rest is sulphate of potash). These factors must be taken into account during the processing of the data. From the reported dose rates in the different blocks (K-block:  $1.38 \text{ Gy/ka}$ , U block:  $13.27 \text{ Gy/ka}$  and Th-block:  $7.10 \text{ Gy/ka}$ ) reported by Rhodes & Schwenninger (2007) and using the dose rate conversion factors of Adamiec & Aitken (1998), Mercier & Falgueres (2007) calculated the effective radionuclide concentrations in the three blocks as 5.7 % of K in the K-block, 117.4 ppm of U in the U-block, and 135.2 ppm of Th and 5.8 ppm of U in the Th-block.

## 2.2 Portable gamma-ray spectrometer

In this study, we have used two sodium iodide (NaI(Tl)) detectors, one supplied by Canberra (Inspector 1000 fitted with a stabilised 2-inch probe) and another by Ortec (Micronomad fitted with a 3-inch probe), to record calibration and field spectra. The Canberra spectrometer saves the spectral and other data (e.g., real-time and live time) in a channel length of 256, 512, 1024, 2048, or 4096 and was used to generate files with a .cnf extension. A MATLAB code was written for extracting the data. The Ortec detector saves data as a file with a .chn extension and in a channel length of 256, 512, 1024, or 2048; all the calibration and field spectra reported in this paper were recorded using this spectrometer. The spectra recorded using the Canberra spectrometer were only used to check or test if OxGamma can read the .cnf file.

## 2.3 MATLAB

The OxGamma application was designed and developed using App Designer, an interactive development environment in MATLAB (MATLAB, 2021). The application package can be

installed and run on both the macOS and Windows platforms without any subscription.

## 2.4 Sample

We have used eighteen field gamma-ray spectra to test the performance of OxGamma. These spectra were collected using the Ortec portable gamma-ray spectrometer and have been previously processed using in-house legacy software. The values of radionuclide (K, U, and Th) concentrations and dose rates, obtained using this in-house software, are listed in Table 1. In addition, for ten of those spectra (i.e., for the samples collected from the same sites), we also have additional ICP-MS results which are listed in the same table.

## 3 Methods

OxGamma provides output using both windows and threshold approaches. The theoretical aspects of both approaches are discussed in the following sections.

### 3.1 The Windows approach

The windows approach is based on the fact that the gamma-ray peak area at a particular energy directly measures the activity and concentration of the radionuclide emitting the gamma-ray at that energy. Such a measurement would be easy if the detector's efficiency were 100%, but, unfortunately, this is not the case. The detector's efficiency is usually significantly lower and it must be calculated at each photon energy. However, since we are interested in a peak area, absolute full-energy peak efficiency is our interest. The absolute full-energy peak efficiency must be calculated with the help of radioactive standard(s) before moving on to processing the spectra from the field. With the efficiency known, one can calculate the activity and concentration of the radionuclide responsible for a peak in the field gamma-ray spectrum using the following equations. According to Gilmore (2008), the activity can be calculated as,

$$A_s = \frac{N}{P_\gamma * \eta} \quad (1)$$

Where,  $A_s$  is the activity of the parent radionuclide in Bq/Kg,  $N$  is the count rate of the peak in

counts per second (cps),  $P_\gamma$  is the emission probability of the gamma rays at the peak energy by parent radionuclide, and  $\eta$  is the detector's efficiency at the same peak position, i.e., full-energy peak efficiency.

With the known  $A_s$ , one can find the radionuclide concentration (Adamiec & Aitken, 1998) as

$$C = \frac{A_s \cdot M \cdot 10^{-3}}{\lambda \cdot N_A \cdot m_s} \quad (2)$$

Where  $C$  is the concentration of the parent radionuclide in parts per million (ppm),  $A_s$  is the activity of the parent radionuclide (Bq/Kg) from equation 1,  $M$  is the atomic weight of the parent radionuclide,  $N_A$  is Avogadro number,  $m_s$  is the mass of the sample in kilograms, and  $\lambda$  is the decay constant of the parent radionuclide. Below are the main steps generally followed during calibration and dose rate determination using the windows approach (Gilmore, 2008).

1. Three regions of interest (windows) around the most distinctive photopeaks representing K, U, and Th radionuclides in the calibration spectra are defined. In the energy range between 0-3 MeV, these peaks appear due to 1460 keV gamma-ray emissions from  $^{40}\text{K}$ , 1760 keV emissions from  $^{214}\text{Bi}$  (U-series), and 2614 keV emissions from  $^{208}\text{Tl}$  (Th-series).
2. Channel to energy calibration is generally obtained by correlating these energies linearly with the corresponding channel numbers in which these emissions peaked.
3. Efficiency calibration is done to evaluate the efficiency of a detector at a given gamma photon energy. The procedure involves finding out two factors: 1) the number of photons observed by the detector ( $N_{obs}$ ) and 2) the number of photons emitted by the gamma source ( $N_{emit}$ ). Then using the following equation, the efficiency as a function of gamma energy can be obtained.

$$\eta = \frac{N_{obs}}{N_{emit}} \quad (3)$$

Where  $N_{obs}$  is the count rate obtained by dividing the total counts in a peak by the measurement time, and  $N_{emit}$  is the product of the activity of the standard source ( $A_b$ )



and the emission probability ( $P_\gamma$ ).

4. This  $\eta$  is fed into equation 1, which involves processing the field spectra and calculating the activity ( $A_s$ ). Afterwards, equation 2 is used to calculate the concentration.

### 3.2 The Threshold approach

This approach is based on finding an energy threshold value above which the spectrum's count rate would be proportional to the gamma dose rate. Thus, it utilises a larger part of the spectrum compared to the windows approach, thereby reducing the measurement time and minimising any effects on the spectrum due to temperature changes during the measurement. For more details on this approach, we may refer to the foundational paper by Murray et al. (1978), Mercier & Falguères (2007) and Duval & Arnold (2013). Here we briefly discuss the methodology as follows.

1. Energy calibration is done in the same way as explained for the windows approach. However, here, no efficiency calibration is required.
2. All the calibration spectra are first normalised to 1000 s and corresponding radionuclide concentrations, 1 % of K, 1 ppm of U, and 1 ppm of Th. Then, the normalised spectra are further normalised by the dose rate conversion factors corresponding to 1 % of K, 1 ppm of U, and 1 ppm of Th.
3. To determine a threshold value, the cumulative spectra are obtained (see Figure 4). The energy at which the relative standard deviation of these spectra reaches a minimum value is noted as a threshold (Figure 4). This energy threshold is then used to find the average detector efficiency factor or n-factor from the cumulative spectra. This n-factor is obtained from the mean value of the  $n_x$  parameters ( $x = K, U, \text{ or } Th$ ), detection efficiencies of the detector or the number of gamma photons recorded in 1000 s corresponding to 1 % of K or 1 ppm of U/Th. Finally, the total gamma dose rate is obtained by dividing the integrated counts in the field spectrum above the same energy threshold by this n-factor.

## 4 Workflow

The general procedure to determine concentrations and dose rates remains the same, irrespective of the calibration standards. However, a few extra steps are always required to be

performed or modified in between. Currently, the OxGamma application can only process the calibration spectra from the Oxford blocks. During the data processing from these blocks, it is necessary to take care of the additional details mentioned in Section 2.1. Figure 1 shows the workflow diagram that OxGamma incorporates; each entity has been discussed as follows.

**Uploading calibration spectra:** The OxGamma application demands four calibration spectra recorded from the four calibration blocks (K, U, Th, and Background; Figure 2). It is capable of processing the spectra in the file format of .cnf, .chn/.Chn or .spe, associated with two of the leading instrument manufacturers (i.e., Mirion/Canberra and Ametec/EG&G Ortec). Alternatively, the spectral data can be imported as an ASCII text file (i.e. .txt). On the main page of the application (left side), by pressing the buttons (K-spectrum, U-spectrum, Th-spectrum, and Background spectrum) one by one, all those spectra can be uploaded, or their path can be inserted into the respective text boxes. Afterwards, the calibrations can be performed in a sequence as Energy → Width → Efficiency. It is to be noted that all the spectra are first smoothened using the Savitzky-Golay filter during processing.

**Energy calibration:** Locating K-, U-, and Th-peak positions is crucial for the channel to energy calibration. Normally, peak-finding algorithms are used to locate these peaks automatically. A single spectrum may contain several peaks and, therefore, OxGamma allows users to only target the peak of their interest. By doing this, it also allows users to set the regions of interest (ROIs or windows i.e. K window, U window, and Th window) at the beginning itself. Now, in these ROIs, users can choose how they would want the peak position to be found- by using Gaussian fitting or by just discovering the maximum point. The former technique requires baseline correction (linear or exponential) and, therefore, users must opt among the choices at the beginning. For example, Figure 3 shows the selected ROI around each peak and gaussian fitting of the peak after subtracting an exponential baseline; an exponential baseline is created with the help of two endpoints in an ROI (Figure 3). A similar procedure is followed when a linear baseline correction is applied (refer to supplementary material 1; Figure S1). However, in the case of no baseline correction, the peak maximum (after spline fitting to the data) corresponds to the maximum count in the ROI - this option is set to default. The option for selecting ROIs appears when pressing the button 'Energy calibration' (see supplementary material 2; Page S2). Please note that working with the fitting methods requires proper

selection of the ROI, which is also important for width calibration. Therefore, users are advised to check Figure S1 carefully to select ROIs properly.

Soon after the choice for baseline correction is made, another pop-up window appears. This window allows users to set ROI or window around the most distinctive photopeaks related to K, U, and Th (Figure S1 and Page S3). During the selection, the software already calculates the peak positions and saves them in the edit boxes at the bottom of the same pop-up window. After all the peak positions get listed, users just need to press 'OK'. By doing this, these values are sent to the text boxes reserved for the channel numbers on the main page of the application (top right), where corresponding energies would be already listed. The procedure ends with the channel to energy calibration by correlating these energies linearly with the corresponding channel numbers. Finally, energy calibration graphs appear in the main application window (see Page S4).

The full width at half maximum (FWHM) is another helpful quantity used for width calibration (see next section) and can be calculated right away from the fitting parameter,  $\sigma$ , the standard deviation, using equation 4. The parameter  $\sigma^2$  corresponds to the variance of the Gaussian distribution.

$$\text{Width (FWHM)} = 2 \sqrt{2 \ln} \cdot \sigma \quad (4)$$

For the technique in which no fitting is used, FWHM is determined by the difference between two points where a horizontal line (through the point at which half of the maximum count occurs) intersects the peak (see Figure S2).

**Width calibration:** The photopeaks in the gamma-ray spectrum are expected to take a Gaussian shape, but their widths (FWHMs) vary with the energy. As the activity or concentration calculation requires the determination of the total counts under these photopeaks (i.e., true peak area), the correct limits of the peak region must be defined beforehand. These limits can be set by estimating FWHM for each photopeak and may not be the same as the ROI defined initially. The FWHM can easily be determined by fitting the peak

with one or more gaussian distribution functions. In principle, the resulting FWHM should be proportional to the energy, and performing a width calibration ensures this relation. Usually, the widths (FWHMs) are retained from the Gaussian fittings performed during energy calibration (see energy calibration).

While defining the limits for a peak, it is important to consider interference from any neighbouring peak(s) and, therefore, checking on the detector's energy resolution is a must. The energy resolution determines its ability to distinguish between two peaks and is obtained from the FWHM of a peak and its centroid using the following equation.

$$\text{Resolution, } R (\%) = \frac{FWHM}{E_c} \cdot 100 \quad (5)$$

Where  $E_c$  is the peak energy. A detector with a higher resolution offers a greater ability to resolve the overlapping peaks and, thereby, helps target the region/peak of interest accurately. For NaI(Tl) detectors, 5-10% of energy resolution is desirable.

OxGamma retains the FWHM values of the K, U, and Th peaks calculated during energy calibration (Page S5). The FWHM set the integration limits for determining the total counts under a peak. It is important to note that the FWHM is considered to set the integration limits in the case of linear or exponential baseline correction. Otherwise, standard limits (peak channel  $\pm 26$  for  $^{40}\text{K}$  and peak channel  $\pm 35$  for  $^{238}\text{U}$  and  $^{232}\text{Th}$ ) are employed assuming energy resolutions between 5-10% (Hossain, 2003). These total counts under each peak are then corrected for background before moving on to the next steps, by employing the spectrum from the BG-block. Note that the K-block is only 72 % concrete and, therefore, the background needs to be adjusted accordingly i.e. 72 % of the background counts. The corrected total counts are then used to determine full-energy peak efficiencies and, later, to calculate stripping factors. The stripping factors are important quantities that determine the actual contribution of individual radionuclides to their own windows; these factors are used in field spectrum stripping to determine actual counts in each of the windows. Since all three radioisotopes contribute to a single spectrum in the field measurement, it is important to strip away any secondary contributions from one radioisotope to the primary peak of another

radioisotope. For more details on the stripping factors and their derivation, we refer to Aitken (1985; Appendix L) and Hossain (2003). During the derivation, using following equation 6, the contribution of U in the Th-block is corrected (Hossain, 2003).

$$C_{Th}^* = C_{Th} - \left( \frac{5.8}{117.4} \right) C_U \quad (6)$$

Here,  $C_{Th}^*$  is the corrected counts in a given peak (K, U, or Th) in the Th-spectrum,  $C_{Th}$  is the counts in the same peak before correction and  $C_U$  is the total counts in the same peak but in the U-spectrum.

**Efficiency calibration:** As discussed previously, three quantities, count rates, emission probabilities, and activities of the parent nuclides, must be known to calculate the peak efficiencies of the detector. The count rate of each peak is calculated by dividing the peak area (see the previous section) by the live time, i.e., actual measurement time. Emission probabilities are standard values and can be found in the book by Gilmore (2008; Appendix D). With these values known, the parent activity of the radionuclide in each block can be calculated from the following equation.

$$A_b = \frac{\lambda \cdot N_A \cdot m_s}{M} \cdot c \cdot 10^{-3} \quad (7)$$

Here,  $A_b$  is the parent activity (in Bq/Kg),  $\lambda$  is the decay constant for the parent nuclide,  $N_A$  is Avogadro's number ( $6.022 \times 10^{23}$ ),  $m_s$  is the mass of the sample in kilograms,  $M$  is the atomic weight of the parent nuclide, and  $c$  is the concentration of the parent nuclide (in ppm). The mass ( $m_s$ ) of each Oxford block has been measured to be 256 kg. The concentrations ( $c$ ) of the parent nuclides in the blocks are 5.7 % of  $^{40}\text{K}$  in K-block, 117.4 ppm of  $^{238}\text{U}$  in U-block, and 135.2 ppm of Th and 5.8 ppm of U in Th-block.

Pressing the button does all the calculations and plots an efficiency calibration curve on the application's main page (Page S5).

**Uploading field spectrum and choosing conversion factors:** After calibration, the field spectrum needs to be uploaded to determine the concentrations and dose rate(s). Users are also required to choose among the conversion factors (Adamiec & Aitken, 1998; Guérin et al., 2012; Liritzis et al., 2013) to convert the concentrations into dose rates (Page S6). At a time, only one spectrum can be processed; a new spectrum can be processed by uploading it again in the same text box (see Figure 1). Please note that there is no need to do calibration every time a new field spectrum is intended to process; the calibration is a one-time process. However, restarting the app resets everything, and users will need to start again.

**Get concentrations and dose rates:** The windows approach push button does all the calculations (see windows approach section) and lists the results in a Table. First, the count rate of a peak in the field spectrum is obtained for the same peak limits as used during efficiency calibration (see the width and efficiency calibration section). These peak limits are channel-based and, therefore, any drift in the field spectra compared to the calibration spectra needs to be corrected beforehand; this is done right after the windows approach button is pushed (Page S7). The drift correction algorithm (Casanovas et al., 2012) aligns the field spectra to the calibration spectra. Once the peak limits are set, the true count rate of each peak is obtained using spectrum stripping. The contribution from the cosmic rays and radioactive impurities in the detector (0.038, 0.014, and 0.019 counts/s for the K, U, and Th windows, respectively) is also adjusted during true count rate determination (Aitken, 1985).

The threshold approach push button performs all the calculations automatically but utilises a different workflow (see threshold approach section). This approach also requires drift correction in the field spectra. The contribution from the cosmic rays and radioactive impurities in the detector here is considered to be 0.01 Gy/ka as observed by Duval & Arnold (2013) and is subtracted from the total gamma dose rate before it is put into the table (Page S9).

The uncertainty in dose rate(s) is obtained through quadrature error propagation involving standard uncertainties in the radionuclide concentrations (i.e., 5%) and uncertainties in the conversion factors from Durcan et al. (2015) and Liritzis et al. (2013). In the case of the threshold approach, a 5% of uncertainty in the total dose rate has been considered.

Supplementary material 2 provides detailed instructions for operating OxGamma (Page S1-S11).

## 5 Tabs

The OxGamma consists of five different tabs. The 'Windows Approach' tab includes results from the calibration process (e.g., spectra, calibration curves, stripping factors) as well as the table containing the concentration of the parent radionuclides (K, U, and Th) and corresponding dose rates. The table also includes the total gamma dose rate value, the sum of individuals, and the total dose rate ( $\beta + \gamma$ ). The 'Threshold Approach' tab includes all the results (e.g., spectra, total dose rate in a table) obtained using the threshold technique. The 'Calibration Report' tab keeps a record of all the parameters that are obtained during the calibration process. The 'Hint' tab includes a brief explanation for the window/spectral range selection procedure and a flow chart. The last tab, Spectrum Viewer, allows users to view and export their spectra; this is an independent tab and requires spectra to be uploaded separately.

## 6 Output

Eighteen field spectra were processed in OxGamma; the results are summarised in Table 2. In the case of the windows approach, gamma dose rates were obtained from the radionuclide concentrations with the help of conversion factors. However, the threshold approach directly resulted in the total gamma dose rate. Figure 5a shows a comparison between dose rates from OxGamma (windows and threshold approaches) and in-house software (windows approach only). Dose rates obtained using the windows approach from both these software mostly agree (Figure 5a). However, a slight difference might be caused by the conversion factors used; OxGamma uses the conversion factors by Adamiec & Aitken (1998) while in-house software used these factors by Nambi & Aitken (1986). Furthermore, gamma dose rates derived using the threshold approach appear to be slightly higher than those obtained via the windows method but are within ~10% of uncertainty (Figure 5b); a similar observation has been reported by Duval & Arnold (2013). These authors found that, on average, the threshold

approach yielded ~4% higher dose rates than the windows approach; for some samples/spectra, the deviation from unity was even up to 12%. They interpreted this deviation as a result of a minor calibration problem in the NaI(Tl) probe or associated error in deriving the n-factor.

We also compared dose rates obtained using OxGamma with the dose rates obtained from the concentrations, which were measured using ICP-MS. For less than 1 Gy/ka dose rate, their relationship appears to be semi-linear (Figure 5c). In some cases, the deviation is greater than 10% from the unity. The reasons for this significant deviation could be: 1) dose rates obtained here using gamma-ray spectrometry have not been corrected for water content, and 2) measurement techniques that differ a lot; ICP-MS determines the concentrations from a definite amount of sediment, and the measurement is done in the lab, whereas, the gamma-ray spectra are measured at the sampling location itself.

## 7 Conclusion

OxGamma, a practical MATLAB-based application compatible with both Windows and macOS, has been developed for practitioners in ESR and luminescence dating to facilitate and simplify the energy, width, and efficiency calibration of portable gamma-ray spectrometers using appropriate standards (U, Th, K & background) to allow for speedy analysis of field spectra and dose rate calculations. In its current version, the application is tailored specifically for use with the Oxford calibration blocks and assumes an infinite matrix geometry. The performance of the software was tested using eighteen field spectra and the concentrations and dose rates were found to be in good agreement with the results obtained independently from existing in-house software and elemental analysis.

**Acknowledgements:** This research was supported by the NERC-funded project NE/T001313/1.

## 8 References

Adamiec, G., & Aitken, M. J. (1998). Dose-rate conversion factors: update. *Ancient TL*, 16,



37–50.

- Aitken, M. J. (1985). *Thermoluminescence dating*. U.S. ed. ed, Studies in archaeological science. Academic Press, London ; Orlando.
- Arnold, L. J., Duval, M., Falguères, C., Bahain, J. J., & Demuro, M. (2012). Portable gamma spectrometry with cerium-doped lanthanum bromide scintillators: Suitability assessments for luminescence and electron spin resonance dating applications. *Radiation Measurements*, 47(1). <https://doi.org/10.1016/j.radmeas.2011.09.001>
- Bates, M., Pope, M., Shaw, A., Scott, B., & Schwenninger, J. L. (2013). Late Neanderthal occupation in North-West Europe: Rediscovery, investigation and dating of a last glacial sediment sequence at the site of La Cotte de Saint Brelade, Jersey. *Journal of Quaternary Science*, 28(7). <https://doi.org/10.1002/jqs.2669>
- Casanovas, R., Morant, J. J., & Salvadó, M. (2012). Temperature peak-shift correction methods for NaI(Tl) and LaBr<sub>3</sub>(Ce) gamma-ray spectrum stabilisation. *Radiation Measurements*, 47(8), 588–595.  
<https://doi.org/https://doi.org/10.1016/j.radmeas.2012.06.001>
- Bowman, S. G. E. (1976). *Thermoluminescent dating: the evaluation of radiation dosage*.
- Durcan, J. A., King, G. E., & Duller, G. A. T. (2015). DRAC: Dose Rate and Age Calculator for trapped charge dating. *Quaternary Geochronology*, 28.  
<https://doi.org/10.1016/j.quageo.2015.03.012>
- Duval, M., & Arnold, L. J. (2013). Field gamma dose-rate assessment in natural sedimentary contexts using LaBr<sub>3</sub>(Ce) and NaI(Tl) probes: A comparison between the “threshold” and “windows” techniques. *Applied Radiation and Isotopes*, 74.  
<https://doi.org/10.1016/j.apradiso.2012.12.006>
- Gilmore, G. R. (2008). *Practical Gamma-ray Spectrometry* (2nd ed.). John Wiley & Sons Ltd.
- Guérin, G., Mercier, N., Nathan, R., Adamiec, G., & Lefrais, Y. (2012). On the use of the infinite matrix assumption and associated concepts: A critical review. *Radiation Measurements*, 47(9), 778–785. <https://doi.org/10.1016/j.radmeas.2012.04.004>
- Hossain, S. M. (2003). *A critical comparison and evaluation of methods for the annual radiation dose determination in the luminescence dating of sediments*.
- Huntley, D. J., Godfrey-Smith, D. I., & Thewalt, M. L. W. (1985). Optical dating of sediments. *Nature*. <https://doi.org/10.1038/313105a0>
- Ikeya M. (1993). New Applications Of Electron Spin Resonance: Dating, Dosimetry And

- Microscopy. In *New Applications Of Electron Spin Resonance: Dating, Dosimetry And Microscopy*. <https://doi.org/10.1142/9789814317214>
- Lebrun, B., Nicolas Frerebeau, Guilhem Paradol, Guillaume Guérin, Norbert Mercier, Chantal Tribolo, Christelle Lahaye, & Magalie Rizza. (2020). Gamma: An R Package for Dose Rate Estimation from In-Situ Gamma-Ray Spectrometry Measurements. *Ancient TL*, 38(2), 1–5.
- Liritzis, I., Stamoulis, K., Papachristodoulou, C., & Ioannides, K. (2013). A re-evaluation of radiation dose-rate conversion factors. In *Mediterranean Archaeology and Archaeometry* (Vol. 13, Issue 3).
- MATLAB (9.10.0 (R2021a)). (2021). The MathWorks Inc.
- Mercier, N., & Falguères, C. (2007). *Field gamma dose-rate measurement with a NaI(Tl) detector: re-evaluation of the “threshold” technique* (Vol. 25, Issue 1). <https://www.researchgate.net/publication/284313107>
- Moska, P., Bluszcz, A., Poreba, G., Tudyka, K., Adamiec, G., Szymak, A., & Przybyła, A. (2021). Luminescence Dating Procedures at the Gliwice Luminescence Dating Laboratory. *Geochronometria*, 48(1). <https://doi.org/10.2478/geochr-2021-0001>
- Murray, A. S. , Bowman, S. G. E. , & Aitken, M. J. (1978). Evaluation of the gamma dose-rate contribution. *PACT*, 2, 84–96.
- Nambi, K. S. V., & Aitken, M. J. (1986). Annual dose conversion factors for TL and ESR dating. *Archaeometry*, 28, 202–205.
- Rhodes, E. J. (2011). Optically stimulated luminescence dating of sediments over the past 200,000 years. *Annual Review of Earth and Planetary Sciences*, 39. <https://doi.org/10.1146/annurev-earth-040610-133425>
- Rhodes, E.J., & Schwenninger, J.-L. (2007). *Dose rates and radioisotope concentrations in the concrete calibration blocks at Oxford* (Vol. 25, Issue 1).

**Figure captions:**

**Figure 1:** Workflow depicting step-by-step process in OxGamma.

**Figure 2:** Calibration spectra (K, U, Th, and BG) recorded for the four calibration blocks at Oxford University. A NaI(Tl) gamma-ray spectrometer from Ortec was used to record these spectra.

**Figure 3:** Region of interest (ROI) in (a) K-spectrum, (b) U-spectrum, and (c) Th-spectrum. OxGamma enables the selection of an ROI by clicking the computer mouse once at each end of a photopeak (1 and 2). (d, e, f) Gaussian peak fitting of K-peak, U-peak, and Th-peak, respectively, after exponential baseline correction.

**Figure 4:** Cumulative spectra derived from the normalised calibration spectra. The cumulative count at any given energy here represents the sum of all the counts above this energy. The relative standard deviation (RSD) of these cumulative spectra is plotted onto the right axis; the energy corresponding to the minimum of this RSD is marked as the energy threshold.

**Figure 5:** (a) Comparison of gamma dose rates obtained using OxGamma and in-house software. Dose rates from in-house software were determined using the windows approach. (b) Comparison of gamma dose rates using the windows and threshold approaches within OxGamma. (c) Comparison of gamma dose rates calculated from the concentrations obtained using OxGamma and ICP-MS. A total of eighteen samples were used to study the comparison.

**Table 1:** Listing of the field spectra, radionuclide concentrations, and dose rates derived from in-house software and ICP-MS analysis. The conversion factors from Adamiec & Aitken (1998) were used to convert the concentrations into dose rates.

	Analysis using in-house legacy software				Elemental analysis using ICP-MS			
Field Spectrum	Radionuclide concentrations from Gamma spectrometer			Gamma dose rate	Radionuclide concentrations			Gamma dose rate
Laboratory code	K (%)	Th (ppm)	U (ppm)	Gy/ka	K (%)	Th (ppm)	U (ppm)	Gy/ka
X2060	1.04	7.62	1.74	0.824 ± 0.041	-	-	-	-
X2608	3.31	6.26	2.79	1.481 ± 0.074	-	-	-	-
X2609	3.36	5.91	4.38	1.665 ± 0.083	-	-	-	-
X2628	1.60	8.15	1.81	0.998 ± 0.050	-	-	-	-
X2976	1.10	14.72	5.61	1.633 ± 0.082	-	-	-	-
X5020	0.47	4.11	1.14	0.459 ± 0.023	0.50	4.20	1.20	0.653 ± 0.027
X5290	2.43	16.48	4.04	1.917 ± 0.096	-	-	-	-
X6099	1.17	7.66	1.80	0.886 ± 0.044	-	-	-	-
X6102	1.28	8.16	2.12	0.963 ± 0.048	-	-	-	-
X7446	0.19	1.54	0.96	0.232 ± 0.012	0.32	1.30	0.90	0.242 ± 0.014
X7448	0.53	2.33	0.72	0.341 ± 0.017	0.40	1.70	0.40	0.223 ± 0.013
X7449	0.37	1.91	0.64	0.264 ± 0.013	0.32	1.70	0.40	0.204 ± 0.013
X7450	0.43	2.41	0.73	0.315 ± 0.016	0.32	1.60	0.60	0.222 ± 0.013
X7451	0.80	4.43	1.23	0.548 ± 0.027	1.09	5.50	1.40	0.684 ± 0.020
X7453	0.93	5.84	1.63	0.699 ± 0.035	1.26	7.20	1.90	0.864 ± 0.024
X7455	0.31	2.57	1.04	0.303 ± 0.015	0.39	3.20	0.90	0.349 ± 0.015
X7457	0.34	2.24	0.83	0.297 ± 0.015	0.60	2.50	0.60	0.332 ± 0.014
X7462	0.24	1.39	0.60	0.190 ± 0.010	0.31	1.30	0.50	0.193 ± 0.013

**Table 2:** Radionuclide concentrations and dose rates from the OxGamma application using the windows and threshold approaches. Please note the threshold approach only delivers dose rate while the windows approach results in concentrations as well as dose rates.

OxGamma						
	(Windows approach)				(Threshold approach)	
Field Spectrum	Radionuclide concentrations			Gamma dose rate	Gamma dose rate	
Laboratory code	K (%)	Th (ppm)	U (ppm)	Gy/ka	Gy/ka	
X2060	0.996	7.598	1.615	0.786 ± 0.024	0.865	± 0.043
X2608	3.281	6.464	2.785	1.420 ± 0.030	1.612	± 0.081
X2609	3.302	5.928	4.331	1.574 ± 0.034	1.800	± 0.090
X2628	1.559	8.460	1.612	0.964 ± 0.026	1.044	± 0.052
X2976	1.118	15.159	5.406	1.604 ± 0.049	1.800	± 0.090
X5020	0.479	4.466	1.112	0.455 ± 0.017	0.513	± 0.026
X5290	2.456	17.929	3.832	1.883 ± 0.051	2.124	± 0.106
X6099	1.168	8.192	1.750	0.872 ± 0.026	0.970	± 0.049
X6102	1.273	8.764	1.930	0.945 ± 0.027	1.030	± 0.052
X7446	0.216	1.644	1.041	0.248 ± 0.014	0.278	± 0.014
X7448	0.586	2.631	0.706	0.347 ± 0.015	0.400	± 0.020
X7449	0.402	2.111	0.651	0.272 ± 0.014	0.322	± 0.016
X7450	0.472	2.704	0.768	0.330 ± 0.015	0.371	± 0.019
X7451	0.878	4.983	1.329	0.601 ± 0.019	0.656	± 0.033
X7453	1.021	6.745	1.722	0.764 ± 0.023	0.855	± 0.043
X7455	0.344	2.948	1.052	0.343 ± 0.015	0.399	± 0.020
X7457	0.372	2.306	0.863	0.298 ± 0.014	0.354	± 0.018
X7462	0.248	1.585	0.604	0.204 ± 0.013	0.222	± 0.011

Figure 1

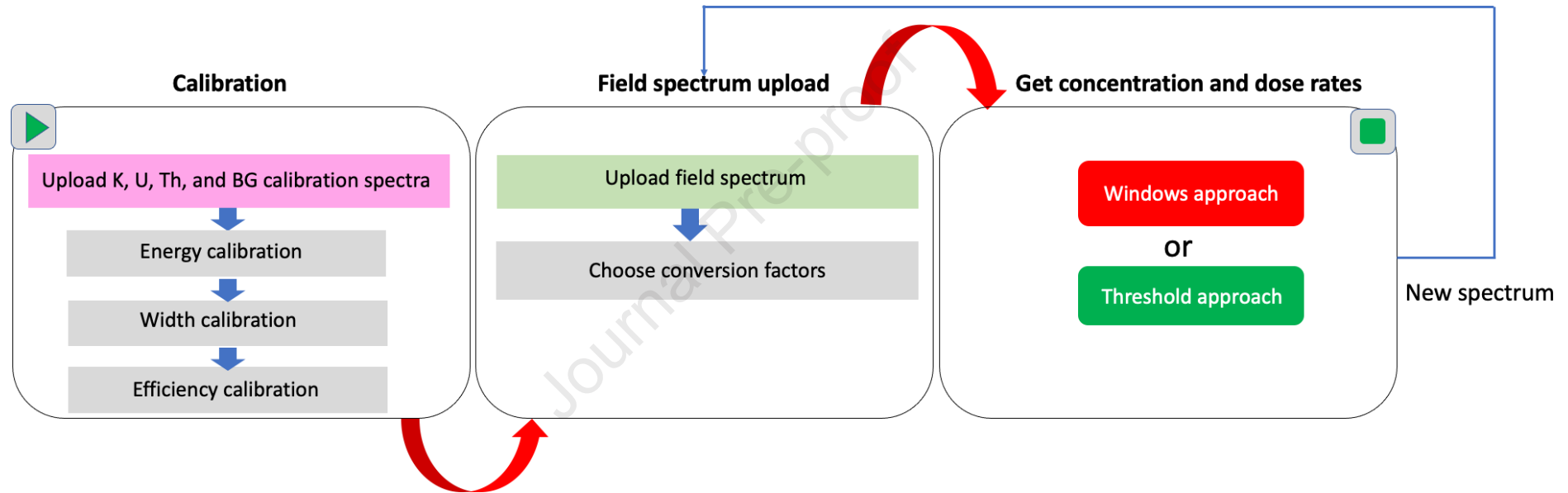


Figure 2

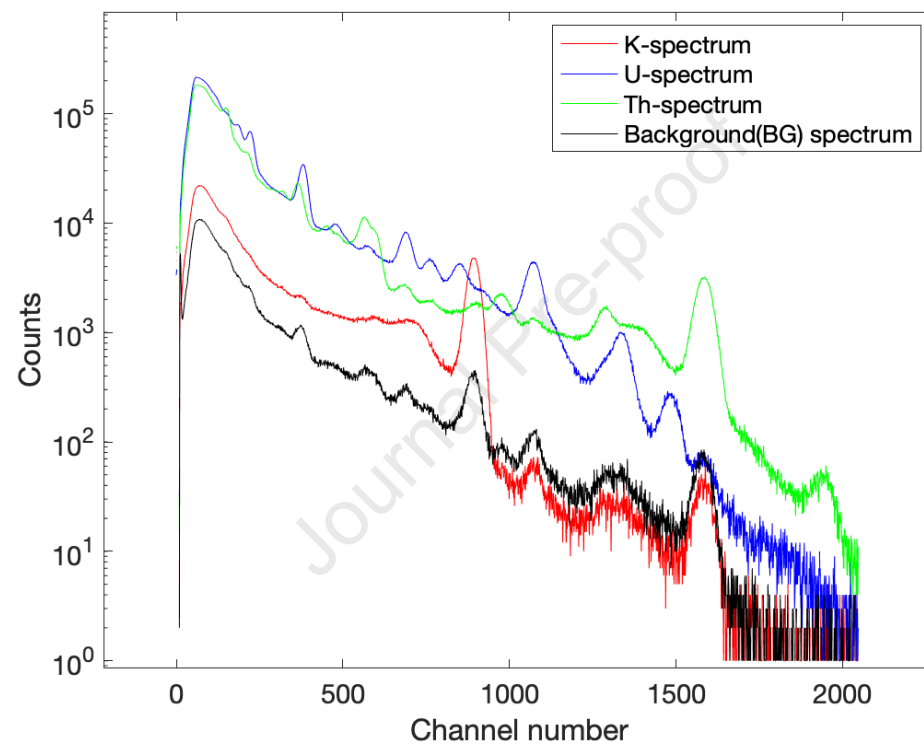


Figure 3

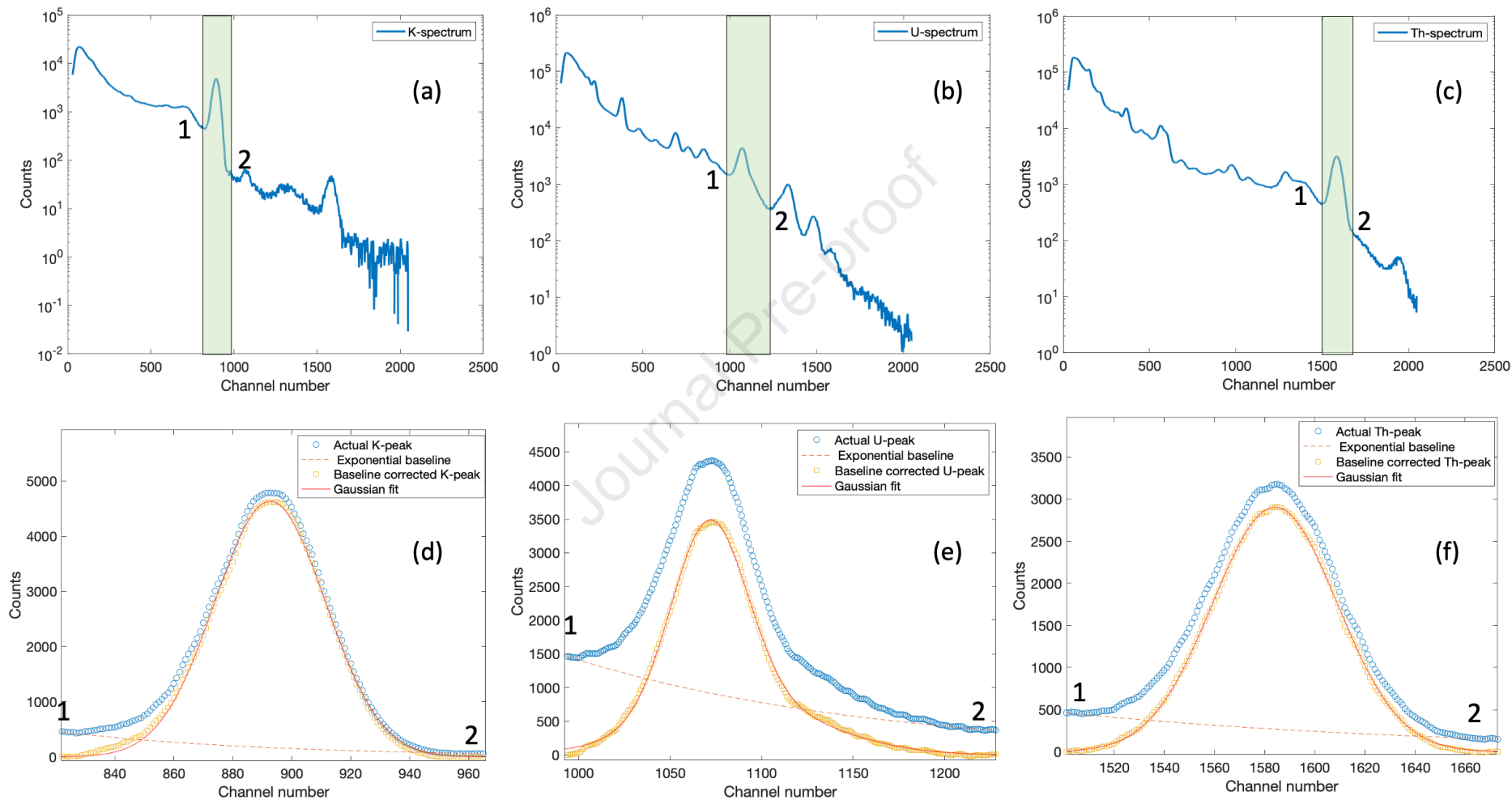




Figure 4

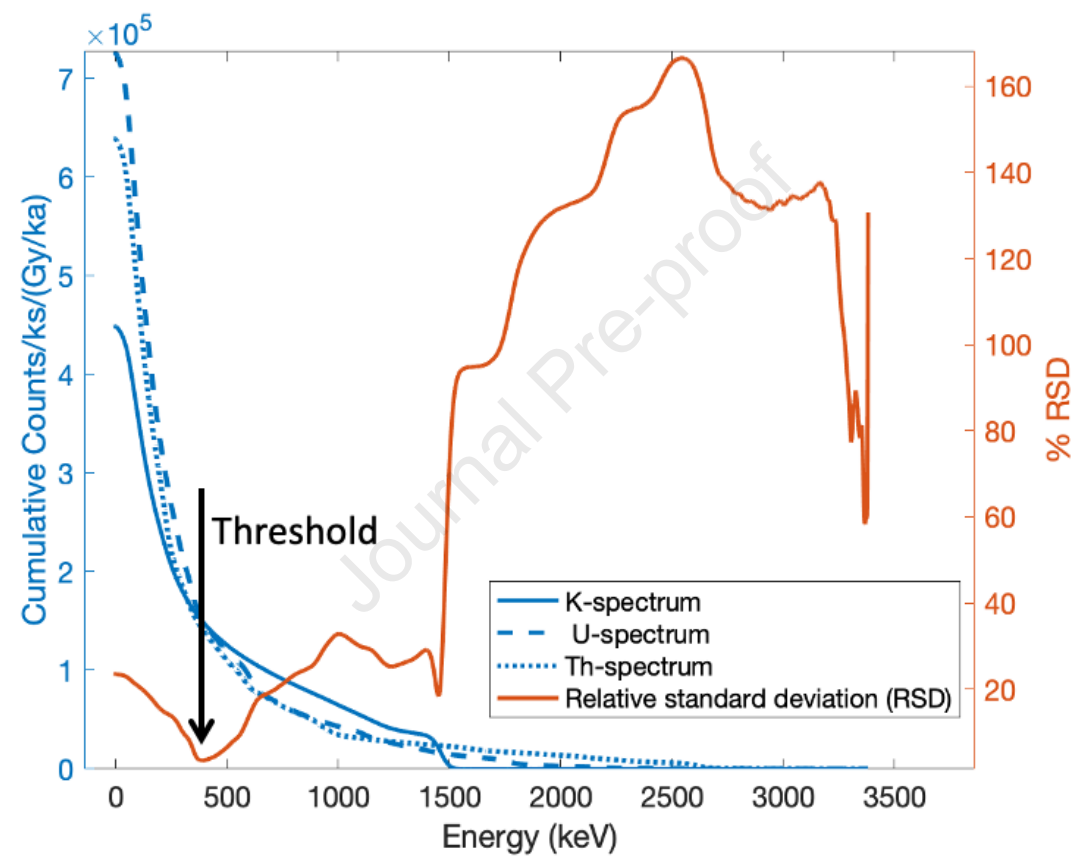
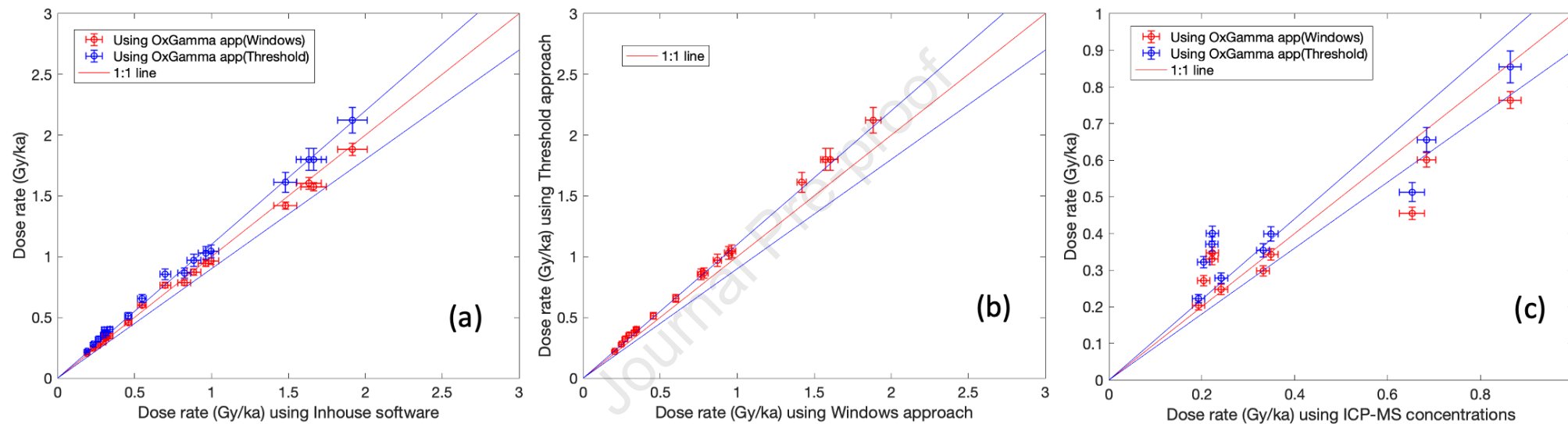


Figure 5



## Highlights

- A MATLAB based application for the calibration of portable gamma-ray spectrometers and the analysis of field spectra for environmental dose-rate measurements.
- Determination of environmental gamma dose rate using windows and threshold techniques.

**Declaration of interests**

☒ The authors declare that they have no known competing financial interests or personal relationships that could have appeared to influence the work reported in this paper.

☐ The authors declare the following financial interests/personal relationships which may be considered as potential competing interests:

--